S100A1 transgenic treatment of acute heart failure causes proteomic changes in rats

YICHEN GUO[1], LIANQUN CUI[1], SHILIANG JIANG[1], DONGMEI WANG[2], SHU JIANG[1], CHEN XIE[1] and YANPING JIA[1]

[1]Department of Cardiology, Shandong Provincial Hospital Affiliated to Shandong University, Jinan, Shandong 250021; [2]Department of Radiology, Shandong Jiao Tong Hospital, Jinan, Shandong 250063, P.R. China

Received May 15, 2015; Accepted March 23, 2016

DOI: 10.3892/mmr.2016.5440

Abstract. S100 Ca^{2+}-binding protein A1 (S100A1) is an important regulator of myocardial contractility. The aim of the present study was to identify the underlying mechanisms of S100A1 activity via profiling the protein expression in rats administered with an S100A1 adenovirus (Ad-S100A1-EGFP) following acute myocardial infarction (AMI). LTQ OrbiTrap mass spectrometry was used to profile the protein expression in the Ad-S100A1-EGFP and control groups post-AMI. Using Protein Analysis Through Evolutionary Relationships (PANTHER) analysis, 134 energy metabolism-associated proteins, which comprised 20 carbohydrate metabolism-associated and 27 lipid metabolism associated proteins, were identified as differentially expressed in the Ad-S100A1-EGFP hearts compared with controls. The majority of the differentially expressed proteins identified were important enzymes involved in energy metabolism. The present study identified 12 Ca^{2+}-binding proteins and 22 cytoskeletal proteins. The majority of the proteins expressed in the Ad-S100A1-EGFP group were upregulated compared with the control group. These results were further validated using western blot analysis. Following AMI, Ca^{2+} is crucial for the recovery of myocardial function in S100A1 transgenic rats as indicated by the upregulation of proteins associated with energy metabolism and Ca^{2+}-binding. Thus, the current study ascertained that energy production and contractile ability were enhanced after AMI in the ventricular myocardium of the Ad-S100A1-EGFP group.

Correspondence to: Professor Lianqun Cui, Department of Cardiology, Shandong Provincial Hospital Affiliated to Shandong University, 324 Jingwuweiqi Road, Jinan, Shandong 250021, P.R. China
E-mail: xc@sdcqm.com.cn

Abbreviations: S100A1, S100 calcium binding protein A1 ISO-OV, isoproterenol overdose; AMI, acute myocardial infarction; PANTHER, Protein Analysis Through Evolutionary Relationships; SERCA2a, sarcoplasmic reticulum ATPase; RyR2, ryanodine receptor 2; EGFP, enhanced green fluorescent protein; LVEDD, left ventricular end-diastolic diameter; LVESD, left ventricular end-systolic diameter; LVPWs, LVPWd, left ventricular systolic and diastolic posterior; LVEF, left ventricular ejection fraction; FS, fractional shortening; cTnI, cardiac troponin I; MLC, myosin light chain; ELC, essential myosin light chain; HSP70, heat shock protein 70

Key words: LTQ OrbiTrap, S100A1 transgenic treatment, calcium, energy metabolism, calcium-binding proteins

Introduction

Cardiovascular disease is a major cause of mortality worldwide and has markedly increased in prevalence. It is characterized by high disability and mortality rates. In a previous study, rats that received an acute isoproterenol overdose (ISO-OV) suffered cardiac apex ischemia-reperfusion damage and arrhythmia, and subsequently underwent cardiac remodeling and dysfunction. At two weeks, myocytes exhibited systolic and diastolic Ca^{2+} mishandling, thus, post-ISO-OV mitochondrial dysfunction may underlie decreased cardiac contractility, ATP depletion and exacerbated oxidative stress (1). S100 Ca^{2+}-binding protein A1 (S100A1) is an important regulator of cardiac function and vascular biology. S100A1 is a Ca^{2+} sensor protein involved in Ca^{2+} signal transduction pathways, and is important for gene expression, secretion, apoptosis, cell differentiation and muscle contraction. S100A1 interacts with the sarcoplasmic reticulum ATPase (SERCA2a) and ryanodine receptor 2 (RyR2), which primarily results in improved Ca^{2+} handling and contractile function (2-5). S100A1 may enhance transient Ca^{2+} amplitudes and decrease diastolic Ca^{2+} overload via increased Ca^{2+}-induced Ca^{2+} release (CICR) from the sarcoplasmic reticulum (SR) and decreased diastolic SR Ca^{2+} leak to improve cardiomyocyte function (2-8). Previously, a mouse model demonstrated that a stable increase in the expression level of Sl00A1 protein significantly enhanced myocardial contractility (9). S100A1 gene knockout mice exhibit acute contractile dysfunction, myocardial apoptosis, early myocardial remodeling, a severely damaged adrenergic signaling system and rapid heart failure (4). In other animal studies, S100A1 gene-targeted therapy reversed experimental heart failure and improved cardiac performance (9,10). However, the understanding how S100A1 effects modifications to cardiac energy metabolism, Ca^{2+}-binding proteins and cytoskeletal proteins following acute myocardial infarction (AMI)

remains relatively limited. LTQ OrbiTrap mass spectrometry is a protein quantification strategy that provides relative and absolute measurements of proteins in complex mixtures (11). The present study used LTQ OrbiTrap mass spectrometry to analyze the expression profiles of energy metabolism-associated proteins, Ca^{2+}-binding proteins and cytoskeletal proteins when S100A1 was overexpressed by an adenovirus following AMI. The current study aims to identify the target proteins that are associated with Ad-S100A1-EGFP following AMI, and finding alternative therapies to reconstitute the energetic state.

Materials and methods

Ethics statement. The current study was conducted with approval from the Ethics Committee of Shandong Provincial Hospital Affiliated to Shandong University (Jinan, Shandong, China).

Adenovirus constructs. The construction of recombinant adenoviruses that carry S100A1 and enhanced green fluorescent protein (EGFP; Ad-S100A1-EGFP), and only EGFP (Ad-EGFP) was performed by Shanghai Jikai Gene Chemical Technology Co., Ltd. (Shanghai, China)

Acute heart failure model. All animal procedures and experiments were performed in accordance with the Guide for the Care and Use of Laboratory Animals published by the US National Institutes of Health (12). A total of 20 male Wistar rats (12-14 weeks old; 250-300 g) were provided by the Experimental Animal Center of Shandong University (Shandong, China). The rats were housed at a constant temperature of 22˚C and a 12-h dark:light cycle. Rats were fed standard laboratory chow and watered *ad libitum*. The animals were randomly divided into 4 groups (3 rats used/time-point) as follows: i) Ad-S100A1-EGFP group, following ligation of the coronary artery for 20 min, $1x10^{10}$ plaque-forming units (pfu) of Ad-S100A1-EGFP in 20 μl were injected into the anterolateral wall of the left ventricle (LV) using a 30-gauge needle; ii) control group, only the coronary artery was ligated without any treatment; iii) Ad-EGFP group, following ligation of the coronary artery for 20 min, $1x10^{10}$ pfu of Ad-EGFP in 20 μl were injected into the anterolateral wall of the LV; and iv) physiological saline group, following ligation of the coronary artery for 20 min, 20 μl physiological saline was injected into the anterolateral wall of the LV.

The rats were anesthetized with an intraperitoneal injection of 30 mg/100 g chloral hydrate and endotracheal intubation was performed. A breathing machine was used to facilitate breathing. The animals were ventilated using an SAR-830/AP small animal ventilator (CWE, Inc., Ardmore, PA, USA) at a rate of 70 breaths per minute. A left thoracotomy was performed between the third-fourth intercostal space and the pericardium was opened. The proximal left anterior descending coronary artery, which is in the left atrium, and the pulmonary arterial cone boundary, 2-3 mm below the left auricle, were encircled and ligated using a 6-0 silk suture. The chest was subsequently closed. A left anterior descending artery ligation in a rat model produces a large area of lateral wall infarction, which may induce acute heart failure.

The rats were euthanized on postoperative days 1, 7 and 14 with an intraperitoneal injection of 40 mg/100 g chloral hydrate. On day 14, acquired echocardiography was performed to obtain the LV end-diastolic diameter (LVEDD), LV end-systolic diameter (LVESD), LV systolic and diastolic posterior (LVPWs and LVPWd, respectively), LV ejection fraction (LVEF) and fractional shortening (FS).

Protein extraction. LV samples (50 mg) were obtained then immediately snap-frozen and stored in liquid nitrogen. The samples were pulverized under liquid nitrogen into a fine powder, which was homogenized in a lysate buffer containing 8 mol/l urea, 1 mol/l dithiothreitol (13) (Roche Diagnostics GmbH, Mannheim, Germany), leupeptinand, aprotinin, pepstatin (all 1 mg/ml), radioimmunoprecipitation assay buffer and 0.1% phenylmethanesulfonyl fluoride (w/v; Sigma-Aldrich, St. Louis, MO, USA) and then lysed on ice for 30 min. The samples were lysed further by sonication for 2 min. The total lysate was centrifuged for 15 min at 4˚C and 10,000-14,000 x g, and the final supernatant was collected.

Sample processing. The protein concentrations of the cleared lysates were then determined using sample processing. Protein extracts (30 μl) were mixed with 200 μl 8 M urea in 0.1 mol/l Tris/HCl (pH 8.5) in a filter unit and centrifuged at 14,000 x g for 15 min, following which the flow-through was discarded from the collection tube. Iodoacetamide solution (0.05 mol/l in urea) was added, then mixed at 600 rpm in a thermo-mixer (Thermo Fisher Scientific, Inc., Waltham, MA, USA) for 1 min and incubated without mixing for 20 min. The filter units were centrifuged at 14,000 x g for 10 min. Urea (100 μl) was added to the filter unit and centrifuged at 14,000 x g for 15 min. This step was repeated twice. NH_4HCO_3 (100 μl 0.05 M in water) was added to the filter unit and centrifuged at 14,000 x g for 10 min. This step was repeated twice. The filter units were transferred to new centrifuge tubes. NH_4HCO_3 (40 μl) and trypsin were added (enzyme-to-protein ratio, 1:100) and mixed at 600 rpm in a thermo-mixer for 1 min. The units were incubated in a wet chamber at 37˚C for 20 h to achieve complete digestion. Subsequently, the filter units were centrifuged again at 14,000 x g for 10 min, and NH_4HCO_3 (40 μl) was added and centrifuged at 14,000 x g for 10 min. The final solution was dried in a vacuum and the samples were stored at -80˚C.

Samples were purified with a C18 column (ReproSil-Pur, Dr. Maisch GmbH, Entringen, Germany). The samples were mixed with 40 μl 0.1% trifluoroacetic acid (TFA) to achieve a pH<4. Acetonitrile (100%, 200 μl) was added to a wet ZipTip and centrifuged at 800 x g for 2 min. This step was repeated twice. A total of 200 μl 0.1% TFA was added to the wet ZipTip and centrifuged at 800 x g for 2 min. This step was repeated twice. The samples were repeatedly drawn 8 times through the ZipTip. The ZipTip was washed twice with 0.1% TFA and centrifuged at 800 x g for 2 min. The peptides were eluted with 40 μl formic acid, dried under a vacuum and stored at -80˚C.

LTQ OrbiTrap. Four injections were made into a NanoLC 1000 (Thermo Fisher Scientific, Inc., Waltham, MA, USA) interfaced to the LTQ OrbiTrap elite mass spectrometer (Thermo Fisher Scientific, Inc.) via a nanosource. The samples were loaded onto a 150 μm x 2 cm peptrap 300 A C18 pre-column

(ReproSil-Pur, Dr. Maisch GmbH) in solvent A (99.9% water/0.1% formic acid) and desalted for 10 min. The peptides were eluted into a 75 μm x 25 cm 100 A C18 analytical column (self-packed; ReproSil-Pur, Dr. Maisch GmbH) and separated with a linear gradient of 5-30% solvent B (99.9% acetonitrile/0.1% formic acid) in 5 min, and then 69% solvent B for 115 min. The flow rate used was 500 nl/min. The survey scans were acquired in the OrbiTrap with a resolving power of 60,000 m/z 400 and an automated gain control target level of $1x10^6$. The 25 most abundant ions were selected for fragmentation using collision-induced dissociation in the linear ion trap. The precursor ions were fragmented with He gas for 30 ms with a normalized collision energy of 35. The dynamic exclusion parameters were set to exclude ions previously selected for fragmentation for 1 min. All data were acquired in reduced profile mode to accommodate further downstream processing.

Protein identification and quantification. Protein identification was accomplished via Proteome Discoverer version 1.4 (Thermo Fisher Scientific, Inc.) and Mascot Server version 2.4 (www.matrixscience.com/server.html). The Mascot search engine was used to identify consolidated data in the Uniprot rat protein database (www.uniprot.org), with carbamidomethylation + 57,005 selected as the fixed modification and oxidation of methionine + 15,995, light-marked dimethylation + 28,0313 (C- and N-terminal) and heavy-marked dimethylation + 32,0564 (C- and N-terminal) set as the variable modifications. The mass tolerance was set to 10 ppm, and the MS/MS tolerance was set to 0.8 Da (14). The trypsin enzymolysis maximum leakage cut-off value was set to 2, and the important threshold value was set to 0.01 to ensure a false discovery rate of <1%. The protein quantification was obtained via unique peptides. $P<0.05$ was considered to indicate a statistically significant difference for protein quantification. To designate significant changes in protein expression, fold changes <2.0 were set as the cut-offs. The analysis was performed twice.

Bioinformatic analyses. Database analyses were performed with Protein Analysis Through Evolutionary Relationships (PANTHERU; www.pantherdb.org) tools. The PANTHER Classification System was designed to classify proteins (and their genes) to facilitate high-throughput analysis.

Western blot analysis. The LTQ OrbiTrap protein expression results were validated using western blot analysis. The total protein extracts used for western blotting were obtained from the described experiments. Protein concentrations were quantified using a BCA Protein Assay kit (Beyotime Institute of Biotechnology, Haimen, China). The samples of 50 μg total proteins were separated using 12% and 10% sodium dodecyl sulfate-polyacrylamide gel electrophoresis (ZSGB-Bio, Beijing, China) and transferred onto polyvinylidene fluoride membranes (Merck Millipore, Darmstadt, Germany) via electro-blotting. The membranes were incubated in TBST containing 5% non-fat dried milk for 1 h at 25˚C. The membranes were then probed with primary mouse monoclonal anti-myosin light chain 3 (MLC3; ab680; Abcam, Cambridge, UK), rabbit polyclonal anti-cardiac troponin I (cTnI; ab47003; Abcam) and rabbit polyclonal anti-heat shock protein 70 (HSP70; 4872S; Cell Signaling Technology, Inc., Danvers, MA, USA) antibodies at 1:1,000 dilution overnight at 4˚C. Horseradish peroxidase-conjugated goat anti-mouse and anti-rabbit antibodies (cat no. SA00001-2; Proteintech Group, Inc., Chicago, IL, USA) were used as the secondary antibodies at a dilution of 1:2,000. Results were visualized with an enhanced chemiluminescence assay (Thermo Fisher Scientific, Inc.). The bands were evaluated by Image J software (version 2.0; National Institutes of Health, Bethesda, MD, USA).Experiments were repeated 3 times)

Immunohistochemical (IHC) staining. The myocardial tissue was fixed in formalin, embedded in conventional paraffin, sectioned (5 μm thickness) and stained using an SP-9001 IHC staining kit (ZSGB-Bio) in accordance with the manufacturer's instructions. The anti-MLC 3 (1:200) and anti-cTnI (1:100) antibodies were incubated with the sections overnight at 4˚C, then incubated at 37˚C for 30 min with biotin-labeled IgG and streptavidin-biotin complex solution. The specimens were stained with 3,3'-diaminobenzidine and counter-stained with hematoxylin. Phosphate-buffered saline was used for the negative control specimens. The specimens were observed and images were captured using a light microscope (Leica DM4000B, Leica Microsystems, Germany, magnification, x400). Brown reaction granules observed in the cells indicated positive staining.

Statistical analysis. One-way analysis of variance was used to determine significant differences between Ad-S100A1-EGFP group and control group, followed by Tukey's multiple comparison test. $P<0.05$ was considered to indicate a statistically significant difference.

Results

Proteomic results. The data from the LTQ OrbiTrap demonstrated that cardiac tissue samples from the Ad-S100A1-EGFP group (day 14) contained 1,507 different proteins. These proteins included well-known markers associated with the cytoskeleton, energy metabolism and actin. In the day 14 control group cardiac tissues, 1,711 proteins were detected, and 1,573 proteins were differentially expressed when the two groups were compared. A 2.0-fold difference in expression was used as the cut-off. Of the differentially expressed proteins, 208 were associated with high-level processes and their biological functions were identified. Metabolism-associated and Ca^{2+}-binding proteins were present in the LV tissue of the Ad-S100A1-EGFP group. Furthermore, searching the protein database revealed that 134 differentially expressed proteins were closely associated with energy metabolism. The majority of proteins were important enzymes involved in energy metabolism. The present study focused on the proteins that were differentially expressed in the Ad-S100A1-EGFP group tissue.

Energy metabolism-associated proteins. Between the Ad-S100A1-EGFP and control groups, 20 distinct carbohydrate metabolism-associated proteins were differentially expressed in the myocardial tissues. There were 6 proteins significantly downregulated in the Ad-S100A1-EGFP group,

Table I. Carbohydrate metabolism-associated proteins differentially expressed in the Ad-S100A1-EGFP group.

Accession	Unique peptide no.	P-value	Fold	Description	Average normalized abundance		Panther protein class
					S100A1	Control	
MDHM_RAT	2	2.00e-002	178.94	Malate dehydrogenase	4.09e+005	2.29e+003	Dehydrogenase
CISY_RAT	2	9.52e-004	4.62	Citrate synthase	1.28e+005	2.77e+004	Transferase lyase
DHSB_RAT	1	3.00e-002	2.58	Succinate dehydrogenase [ubiquinone] iron-sulfur subunit	6.30e+004	2.44e+004	Dehydrogenase
HXK1_RAT	3	1.38e-004	2.22	Hexokinase-1	5.97e+005	2.68e+005	Carbohydrate kinase
KPB1_RAT	2	1.00e-002	2.02	Phosphorylase b kinase regulatory subunit alpha, skeletal muscle isoform	4.99e+004	2.46e+004	Kinase activator
MCCA_RAT	2	3.07e-003	2.55	Methylcrotonoyl-CoA carboxylase subunit alpha	3.23e+006	1.26e+006	Ligase
HCDH_RAT	2	2.00e-002	20.50	Hydroxyacyl-coenzyme A dehydrogenase,	2.88e+005	1.40e+004	Dehydrogenase hydratase epimerase/racemase
PYC_RAT	2	2.00e-002	2.04	Pyruvate carboxylase	6.61e+004	3.24e+004	Ligase
FUMH_RAT	4	3.66e-003	5.18	Fumarate hydratase	6.42e+004	1.24e+004	Hydratase
UD2B2_RAT	1	6.18e-004	2.69	UDP-glucuronos yltransferase 2B2	2.82e+004	1.05e+004	Glycosyltransferase
G3P_RAT	5	1.02e-006	-4.80	Glyceraldehyde-3-phosphate dehydrogenase	3.10e+005	1.49e+006	Dehydrogenase
PCCA_RAT	5	5.17e-003	2.20	Propionyl-CoA carboxylase alpha chain	5.43e+005	2.46e+005	Ligase
K6PF_RAT	3	2.81e-004	3.01	6-phosphofructokinase, muscle type	1.48e+005	4.92e+004	Carbohydrate kinase
PCKGC_RAT	4	2.78e-003	3.09	Phosphoenolpyruvate carboxykinase, cytosolic	1.49e+006	4.83e+005	Decarboxylase
HCDH_RAT	2	2.00e-002	20.50	Hydroxyacyl-coenzyme A dehydrogenase	2.88e+005	1.40e+004	Dehydrogenase
DO2_RAT	2	1.16e-003	-5.27	Dihydrolipoyllysine-residue succinyltransferase component of 2-oxoglutarate dehydrogenase complex	5.42e+003	2.86e+004	Acetyltransferase

Table I. Continued.

Accession	Unique peptide no.	P-value	Fold	Description	Average normalized abundance		Panther protein class
					S100A1	Control	
ECHM_RAT	1	3.08e-004	-20.17	Enoyl-CoA hydratase,	3971.92	8.01e+004	Acetyltransferase
NSDHL_RAT	2	5.65e-005	-41.27	Sterol-4-alpha-carboxylate 3-dehydrogenase, decarboxylating	2306.09	9.52e+004	Oxidoreductase
SCOT1_RAT	3	6.50e-004	-2.41	Succinyl-CoA:3-ketoacid-coenzyme A transferase 1	2.42e+005	5.83e+005	Epimerase/racemase transferase
ECHA_RAT	3	3.67e-004	-4.18	Trifunctional enzyme subunit alpha	2.97e+004	1.24e+005	Dehydrogenase

whereas 14 proteins were upregulated in the Ad-S100A1-EGFP group. The majority of the upregulated proteins were enzymes involved in glycolysis and the tricarboxylic acid cycle, including citrate synthase, succinate dehydrogenase (ubiquinone) iron-sulfur subunit, fumarate hydratase and malate dehydrogenase. These important enzymes limit the catabolism of carbohydrate and energy support (Table I).

Regarding the 27 proteins involved in lipid metabolism, 16 distinct proteins in the myocardial tissue were significantly upregulated in the Ad-S100A1-EGFP group. The upregulated proteins were associated with the following PANTHER classes: reductase, synthesis, transferase, ligase and lyase ribosomal protein (Table II).

The current study identified 14 stimuli response proteins, and 12 differentially expressed proteins that were upregulated in the Ad-S100A1-EGFP group compared with the control group. The majority of the upregulated proteins were important for ATP binding, ATPase activity, the stress response, the immune response and potassium channel activity. Although downregulated proteins were observed, the number was low compared with the upregulated proteins. There were 2 proteins significantly downregulated in the Ad-S100A1-EGFP group, whereas 12 proteins were upregulated (Table III).

The present study identified 12 Ca^{2+}-binding proteins; 7 were upregulated and 5 downregulated in the Ad-S100A1 EGFP group compared with the control group. The majority of the upregulated proteins were important for cardiac muscle contraction, muscle filament sliding and vascular tone modulation. The present study identified 12 Ca^{2+} binding proteins; 7 were upregulated and 5 were downregulated in the Ad-S100A1 EGFP group compared with the control group (Table IV). The majority of the upregulated proteins were important for cardiac muscle contraction, muscle filament sliding and vascular tone modulation.

The current study identified 22 cytoskeletal proteins, 16 of which were upregulated in the Ad-S100A1-EGFP group compared with the control group. The majority of the upregulated proteins were involved in electron transport during muscle contraction, cellular Ca^{2+} ion homeostasis, actin filament capping, actin filament severing and actin filament polymerization. Although downregulated proteins were identified, there were fewer compared with the upregulated proteins. Compared with the control group, 6 proteins were downregulated in the Ad-S100A1-EGFP group, whereas 16 proteins were upregulated (Table V).

MLC 3, cTnI and HSP70. The 218 identified proteins were associated with the cytoskeleton, Ca^{2+}-binding, cellular protein modifications, translation, catalytic activity, apoptosis, biological regulation and energy metabolism. The identified proteins included cTnI, MLC 3 and HSP70. Western blot analysis was performed to further validate the distribution of these proteins in the myocardial tissues of the Ad-S100A1-EGFP and control groups. The changes in the protein levels of cTnI (Fig. 1), MLC 3 (Fig. 2) and HSP70 (Fig. 3) were determined using western blot analysis. The western blot results were generally consistent with the changes detected by LTQ OrbiTrap. All proteomic experiments were performed at least twice to validate the reliability of the LTQ OrbiTrap results. Thus, the present proteomics data are reliable.

Table II. Lipid metabolism-associated proteins differentially expressed in the Ad-S100A1-EGFP group.

Accession	Unique peptides	P-value	Fold	Description	Average normalized abundance		Panther protein class
					S100A1	Control	
DHRS4_RAT	3	9.90e-004	2.42	Dehydrogenase/reductase SDR family member 4	4.64e+005	1.92e+005	Dehydrogenase
ACSL5_RAT	3	2.00e-002	2.04	Long-chain-fatty-acid-CoA ligase 5	7.54e+005	3.71e+005	Ligase
HMCS1_RAT	2	2.00e-002	4.60	Hydroxymethylglutaryl-CoA synthase	7.58e+005	1.65e+005	Transferase
ACADM_RAT	2	1.64e-003	2.93	Medium-chain specific acyl-CoA dehydrogenase	1.20e+005	4.10e+004	Transferase
MCCA_RAT	2	3.07e-003	2.55	Methylcrotonoyl-CoA carboxylase subunit alpha	3.23e+006	1.26e+006	Ligase
CAV3_RAT	1	2.34e-004	3.44	Caveolin-3	7.31e+005	2.13e+005	Transmembrane receptor regulatory/adaptor protein
HCDH_RAT	2	2.00e-002	20.50	Hydroxyacyl-coenzyme A dehydrogenase,	2.88e+005	1.40e+004	Dehydrogenase hydratase epimerase/racemase
MCAT_RAT	2	6.06e-003	2.05	Mitochondrial carnitine/acylcarnitine carrier protein	2.61e+005	1.28e+005	Amino acid transporter
ACSF2_RAT	4	4.81e-004	2.84	Acyl-CoA synthetase family member2	2.69e+005	9.47e+004	Dehydrogenase
CAV1_RAT	2	2.00e-002	2.12	Caveolin-1	2.96e+005	1.39e+005	Transmembrane receptor regulatory/adaptor protein
ECHP_RAT	3	4.82e-004	2.35	Peroxisomal bifunctional enzyme	2.25e+005	9.55e+004	Dehydrogenase
RL8_RAT	1	8.22e-003	3.07	60S ribosomal protein L8	9.43e+004	3.07e+004	Ribosomal protein
PYC_RAT	2	2.00e-002	2.04	Pyruvate carboxylase, mitochondrial	6.61e+004	3.24e+004	Ligase
UD2B2_RAT	1	6.18e-004	2.69	UDP-glucuronos yltransferase 2B2	2.82e+004	1.05e+004	glycosyltransferase
PCCA_RAT	1	5.17e-003	2.20	Propionyl-CoA carboxylase alpha chain, mitochondrial	5.43e+005	2.46e+005	Ligase
DECR_RAT	7	3.29e-004	2.92	2,4-dienoyl-CoA reductase	1.16e+006	3.98e+005	Dehydrogenase
LBR_RAT	1	2.80e-003	-468.97	Lamin-B receptor	4.45	2.09e+003	Receptor
ADT1_RAT	1	9.97e-006	-11.39	ADP/ATP translocase 1	6.63e+004	7.55e+005	Amino acid transporter
ECHM_RAT	1	3.08e-004	-20.17	Enoyl-CoA hydratase, mitochondrial	3971.92	8.01e+004	Acetyltransferase
NSDHL_RAT	2	5.65e-005	-41.27	Sterol-4-alpha-carboxylate 3-dehydrogenase, decarboxylating	2306.09	9.52e+004	Oxidoreductase
ECHA_RAT	3	3.67e-004	-4.18	Trifunctional enzyme subunit alpha	2.97e+004	1.24e+005	Dehydrogenase
ETFA_RAT	3	2.00e-002	-3.17	Electron transfer flavoprotein subunit alpha	1.14e+004	3.63e+004	Epimerase/racemase transferase
FAS_RAT	1	3.80e-005	-∞	Fatty acid synthase	0.00	602.35	Acyltransferase
SCOT1_RAT	3	6.50e-004	-2.41	Succinyl-CoA:3-ketoacid-coenzyme A transferase 1	2.42e+005	5.83e+005	Epimerase/racemase transferase
CDS2_RAT	1	7.24e-007	-∞	Phosphatidate cytidylyltransferase 2	0.00	2749.92	Nucleotidytranferase
ACADL_RAT	4	8.86e-004	-2.06	Long-chain specific acyl-CoA dehydrogenase	5.98e+004	1.23e+005	Transferase
MPCP_RAT	6	6.45e-008	-2.36	Phosphate carrier protein	4.93e+005	1.17e+006	Amino acid transporter

Table III. Response to stimulus proteins differentially expressed in the Ad-S100A1-EGFP group.

Accession	Unique peptide no.	P-value	Fold	Description	Average normalized abundance		Panther protein class
					S100A1	Control	
CTP5B_RAT	1	2.00e-002	367.49	Contactin-associated protein like 5-2	4.28e+005	1.17e+003	Transporter
ABCC9_RAT	1	2.64e-006	5.97	ATP-binding cassette sub-family C member 9	7.53e+004	1.26e+004	ATP-binding cassette (ABC) transporter
MSH2_RAT	4	2.68e-003	3.62	DNA mismatch repair protein Msh2	2.72e+005	7.53e+004	DNA binding protein
HRH4_RAT	1	4.85e-005	3.51	Histamine H4 receptor	1.59e+005	4.51e+004	G-protein coupled receptor
GPR37_RAT	3	2.10e-003	2.24	Probable G-protein coupled receptor 37	1.12e+005	4.99e+004	G-protein coupled receptor
CO1A2_RAT	4	2.33e-005	2.27	Collagen alpha-2(I) chain	6.43e+005	2.84e+005	Transporter
CO8B_RAT	2	5.12e-003	2.13	Complement component C8 beta chain	2.07e+005	9.75e+004	Apolipoprotein
COBA1_RAT	3	1.00e-002	2.24	Collagen alpha-1(XI) chain	6.35e+004	2.83e+004	Transporter
PLAK_RAT	2	5.00e-002	10.52	Junction plakoglobin	8.56e+004	8.14e+003	Signaling molecule
RBM43_RAT	1	1.00e-002	2.27	RNA-binding protein 43	1.24e+005	5.46e+004	Transcription cofactor
CSF1_RAT	1	1.05e-003	3.81	Macrophage colony-stimulating factor 1	2.69e+004	7.054e+003	Cytokine
HSP74_RAT	2	1.95e-003	2.27	Heat shock 70 kDa protein 4	9.09e+004	4.01e+004	Hsp70 family chaperone
APOH_RAT	1	7.98e-003	-15.96	Beta-2-glycoprotein 1	2.38e+003	3.80e+004	Apolipoprotein
MK13_RAT	3	2.00e-002	-4.46	Mitogen-activated protein kinase 13	8.47e+004	3.78e+005	No-receptor serine/ threonine protein kinase

Table IV. Calcium-binding proteins differentially expressed in the Ad-S100A1-EGFP group.

Accession	Unique peptide no.	P-value	Fold	Description	Average normalized abundance		Panther protein class
					S100A1	Control	
EFHD2_RAT	1	5.69e-003	2.49	EF-hand domain-containing protein D2	2.68e+005	1.07e+005	Calcium-binding protein
MCAT_RAT	2	6.06e-003	2.05	Mitochondrial carnitine/acylcarnitine carrier protein	2.61e+005	1.28e+005	Mitochondrial carrier protein transfer/carrier protein calmodulin
NELL1_RAT	1	5.57e-003	3.95	Protein kinase C-binding protein NELL1	6.33e+005	1.60e+005	Calmodulin
SPT21_RAT	2	2.00e-002	2.40	Spermatogenesis-associated protein 21	3.50e+005	1.46e+005	Calmodulin
GELS_RAT	3	9.93e-005	4.15	Gelsolin	6.52e+005	1.57e+005	Calcium-binding protein
EHD1_RAT	1	4.66e-004	2.13	EH domain-containing protein 1	2.08e+004	9.78e+003	Calcium-binding protein
GPAT3_RAT	1	2.00e-002	5.12	Glycerol-3-phosphate acyltransferase 3	1.12e+004	2.18e+003	Calmodulin
CALL3_RAT	1	9.19e-005	-4.37	Calmodulin-like protein 3	4.11e+004	1.80e+005	Calmodulin
MYL3_RAT	4	1.07e-004	-4.43	Myosin light chain 3	3.23e+005	1.43e+006	Calmodulin
CALX_RAT	3	8.97e-003	-7.48	Calnexin	1.11e+004	8.31e+004	Calcium-binding protein
ADT1_RAT	1	9.97e-006	-11.39	ADP/ATP translocase 1	6.63e+004	7.55e+005	Amino acid transporter
MPCP_RAT	6	6.45e-008	-2.36	Phosphate caaarrier protein	4.93e+005	1.17e+006	Mitochondrial carrier protein transfer/carrier protein calmodulin

Table V. Cytoskeletal proteins differentially expressed in the Ad-S100A1-EGFP group.

Accession	Unique peptide no.	P-value	Fold	Description	Average normalized abundance		Panther protein class
					S100A1	Control	
MARE3_RAT	1	3.36e-003	2.32	Microtubule-associated protein RP/EB family member 3	2.97e+005	1.28e+005	Non-motor microtubule binding protein
TNNI3_RAT	2	1.01e-003	2.95	Troponin I, cardiac muscle	9.94e+005	3.37e+005	Non-motor actin binding protein
CALD1_RAT	4	6.72e-004	2.07	Non-muscle caldesmon	2.96e+005	1.43e+005	Non-motor actin binding protein
MYBPH_RAT	1	3.00e-002	2.28	Myosin-binding protein H	1.98e+005	8.68e+004	Non-reporter serine/ threonine protein kinase
MYPC_RAT	1	9.94e-003	2.22	Myosin-binding protein C, cardiac-type	2.73e+006	1.23e+006	Non-reporter serine/ threonine protein kinase
KIF1C_RAT	4	8.37e-003	2.14	Kinesin-like protein KIF1C	1.37e+005	6.40e+004	Microtubule binding motor protein
KIF22_RAT	2	9.43e-003	2.24	Kinesin-like protein KIF22	1.64e+004	7287.25	Microtubule binding motor protein
TBA1A_RAT	1	9.20e-004	2.91	Tubulin alpha-1A chain	1.98e+005	6.81e+004	tubulin
ABLM2_RAT	2	6.67e-003	3.53	Actin-binding LIM protein 2	6.01e+004	1.70e+004	Structural protein
MYH3_RAT	5	3.06e-003	2.35	Myosin-3	1.93e+005	8.21e+004	Actin binding motor protein
PLAK_RAT	2	5.00e-002	10.52	Junction plakoglobin	8.56e+004	8141.00	Cytoskeletal protein
ARP2_RAT	2	3.37e-003	2.11	Actin-related protein 2	6.08e+004	2.88e+004	Actin and actin related protein
CAPZB_RAT	1	1.78e-004	3.58	F-actin-capping protein subunit beta	4.29e+004	1.20e+004	Non-motor actin binding protein
GELS_RAT	3	9.93e-005	4.15	Gelsolin	6.52e+005	1.57e+005	Calcium-binding protein
LMNA_RAT	3	4.88e-003	2.60	Prelamin-A/ C	1.28e+005	4.94e+004	Structural protein
MYH11_RAT	2	1.94e-003	2.86	Myosin-11 (Fragments)	5.37e+005	1.88e+005	Actin binding motor protein
MYL3_RAT	4	1.07e-004	-4.43	Myosin light chain 3	3.23e+005	1.43e+006	calmodulin
TPM1_RAT	3	5.62e-006	-3.46	Tropomyosin alpha-1 chain	7.44e+005	2.57e+006	Actin binding motor protein

Table V. Continued.

Accession	Unique peptide no.	P-value	Fold	Description	Average normalized abundance		Panther protein class
					S100A1	Control	
ACTB_RAT	2	9.32e-005	-18.34	Actin, cytoplasmic 1	1955.75	3.59e+004	Actin and actin related protein
GFAP_RAT	2	6.29e-003	-7.03	Glial fibrillary acidic protein	2342.24	1.65e+004	Structural protein
MACF1_RAT	4	1.69e-003	-2.39	Microtubule-actin cross-linking factor 1	2.28e+004	5.45e+004	Non-motor actin binding protein
MARK2_RAT	1	8.36e-003	-2.77	Serine/threonine-protein kinase MARK2	1.07e+005	2.98e+005	No-receptor serine/ threonine protein kinase

IHC analysis. Fig. 4 demonstrates positive immunoreactions for the different markers (cTnI, MLC 3 and HSP70) analyzed in the Ad-S100A1-EGFP and control myocardial tissues. The IHC results demonstrated that the proteins were localized to the cytoplasm and nucleus of myocardial cells. Compared with the control group, expression of cTnI and HSP70 was increased in the cytoplasm of the Ad-S100A1-EGFP group. By contrast, cytoplasmic MLC 3 expression was higher in the control group compared with the Ad-S100A1-EGFP group.

Discussion

Main finding. The main finding of the current proteomics study is that the majority of the differentially expressed proteins identified were upregulated in the Ad-S100A1-EGFP group compared with the control group. Additionally, the majority of proteins were important enzymes involved in energy metabolism. In the Ad-S100A1-EGFP group, various Ca^{2+}-binding and cytoskeletal proteins were upregulated. These findings suggest that energy production status and cardiac muscle contraction are important for the recovery of cardiac function.

The present study successfully identified and analyzed the protein profile of Ad-S100A1-EGFP group rats. To the best of our knowledge, this is the first study to analyze the protein profile of rats administered with Ad-S100A1-EGFP adenovirus using LTQ OrbiTrap.

Proteomics and energy metabolism status in the Ad-S100A1-EGFP group. According to the PANTHER classification used in the present study, energy metabolism status and cardiac muscle contraction are important factors in during cardiac function recovery following acute heart failure. Furthermore, previous experimental data suggest a close association between LV remodeling, energy metabolism status and acute heart failure (15). Compared with the control group, 14 carbohydrate metabolism-associated proteins were upregulated in the Ad-S100A1-EGFP group, including malate dehydrogenase, citrate synthase, succinate dehydrogenase (ubiquinone) iron-sulfur subunit, fumarate hydratase hexokinase-1, 6-phosphofructokinase, phosphorylase b kinase regulatory subunit alpha, phosphoenolpyruvate carboxykinase and UDP-glucuronosyl transferase 2B2. Additionally, a number of the significantly upregulated proteins were important enzymes involved in glycolysis and the tricarboxylic acid cycle. These findings indicate that carbohydrate anabolism was upregulated in the Ad-S100A1-EGFP group. The heart is an absolute aerobic organ, thus the majority of the energy required for its activity is obtained from the aerobic oxidation of fatty acids and competing energy substrates (including glucose, ketones, lactate and amino acids). It is understood that there is a clear decrease in fatty acid oxidation capacity during advanced heart failure and glucose uptake is doubled compared with controls. Given that optimal cardiac function under normal and pathological conditions is dependent on glycolysis and pyruvate oxidation (13), the increase in carbohydrate metabolism-associated proteins may also contribute to the increased ventricular contractility in the Ad-S100A1-EGFP group. Of the differentially expressed proteins involved in lipid metabolism, 16 proteins were upregulated, which suggests lipid metabolism was increased

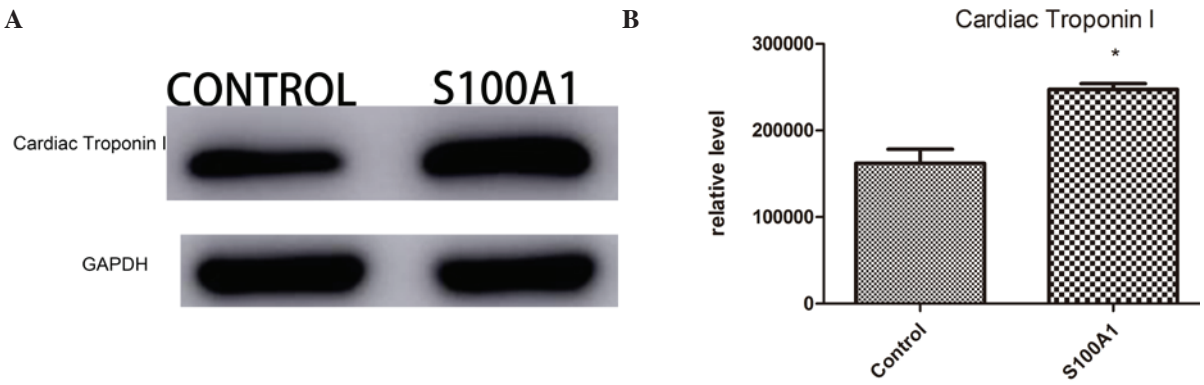

Figure 1. (A) Western blot analysis of the cardiac troponin I expression in the left ventricular tissue from the Ad-S100A1-EGFP and control groups. (B) Relative cardiac troponin I levels measured via western blotting. *P<0.01 vs. control. S100A1, S100 calcium binding protein A1; GAPDH, glyceraldehyde 3-phosphate dehydrogenase.

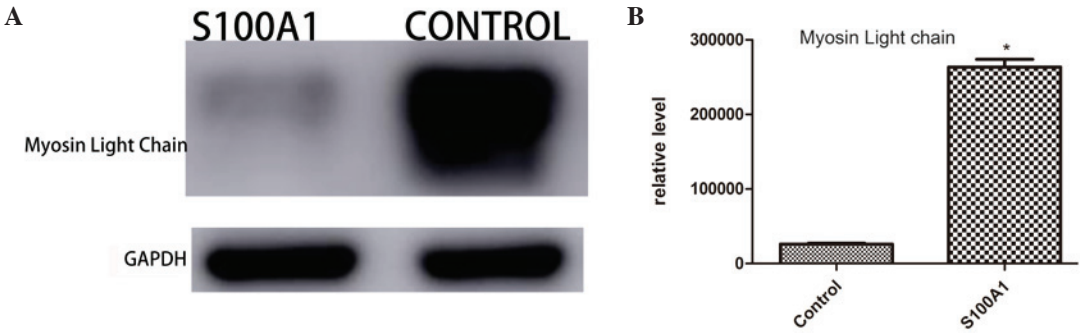

Figure 2. (A) Western blot analysis of the myosin light chain 3 expression in the left ventricular tissue from the Ad-S100A1-EGFP and control groups. (B) Relative levels of myosin light chain 3 measured via western blotting. *P<0.01 vs. control. S100A1, S100 calcium binding protein A1; GAPDH, glyceraldehyde 3-phosphate dehydrogenase.

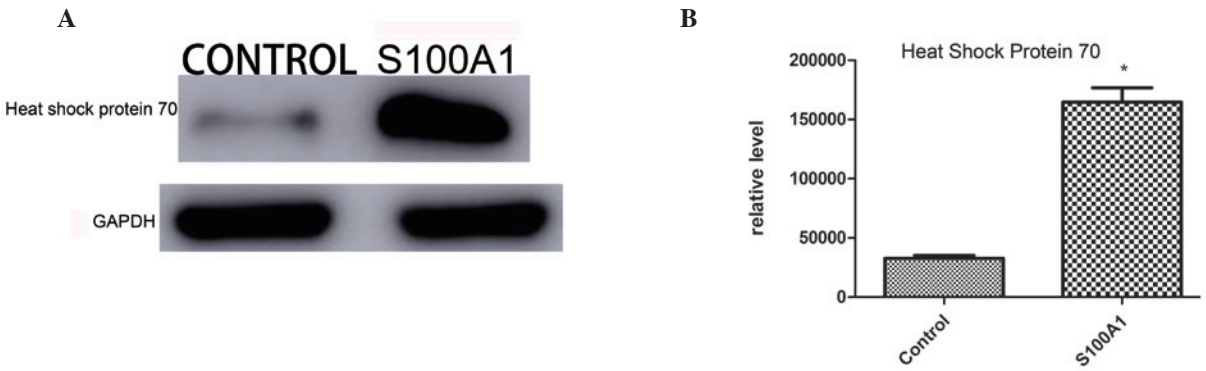

Figure 3. (A) Western blot of the heat shock protein 70 expression in the left ventricular tissue from the Ad-S100A1-EGFP and control groups. (B) Relative levels measured via western blotting. *P<0.01 vs. control. S100A1, S100 calcium binding protein A1; GAPDH, glyceraldehyde 3-phosphate dehydrogenase.

in the Ad-S100A1-EGFP group. Furthermore, these upregulated proteins had closely associated functions, particularly long-chain-fatty-acid-CoA ligase 5, which is crucial for the regulation of lipid metabolism. In addition, the functions of these proteins in fatty acid oxidative metabolism may exert an important effect on cardiomyocyte energy supply. Fatty acid β-oxidation involves four enzymes (acyl CoA dehydrogenase, 2,3 enoyl CoA hydratase, 3-OH acyl CoA dehydrogenase and 3-keotacyl CoA thiolase) (15). The proteomic screening in the present study detected the expression of acyl-CoA dehydrogenase (medium-chain and long-chain), enoyl CoA hydratase and hydroxyacyl CoA dehydrogenase. Among these proteins, acyl-CoA dehydrogenase (medium-chain) and hydroxyacyl CoA dehydrogenase were significantly upregulated in the Ad-S100A1-EGFP group compared with the control group. 2,4-dienoyl CoA reductase is the auxiliary enzyme for fatty acid β-oxidation and acyl-CoA dehydrogenase catalyzes the initial rate-limiting step in mitochondrial fatty acid β-oxidation (16). Hydroxyacyl-coenzyme A dehydrogenase is essential for the mitochondrial β-oxidation of

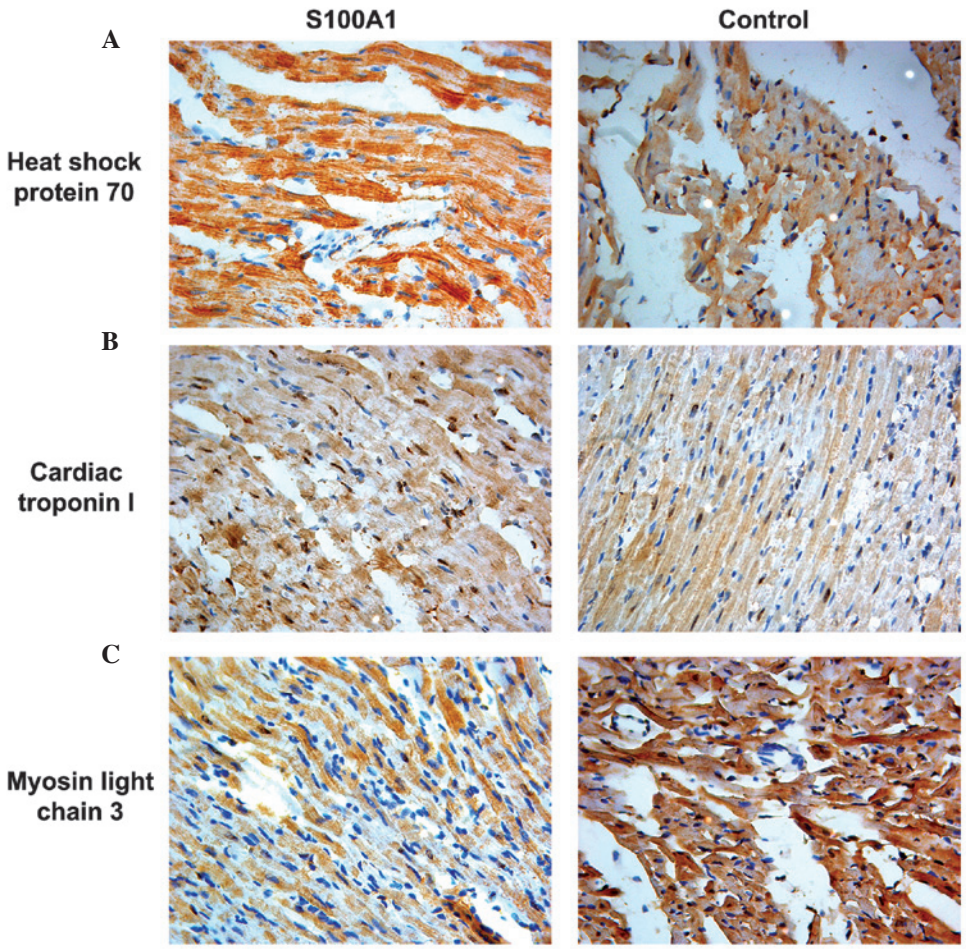

Figure 4. Immunohistochemical analysis of the myocardial tissue. Expression of (A) heat shock protein 70, (B) cardiac troponin I and (C) myosin light chain 3 were examined in Ad-S100A1-EGFP and control group tissues. Magnification, x400.

short chain fatty acids and it exerts its highest activity toward 3-hydroxybutyryl-CoA. The upregulation of acyl-CoA dehydrogenase and hydroxyacyl-coenzyme A dehydrogenase in the ventricular tissue of Ad-S100A1-EGFP group rats may be beneficial for myocardial function. Oxidative phosphorylation is the principal process by which ATP is formed (17). Changes in the expression of enzymes involved in respiratory chain complexes may impair energy production in myocytes. Various modifications to energy metabolism were demonstrated in the Ad-S100A1-EGFP group. The current study demonstrated that many proteins were upregulated in the Ad-S100A1-EGFP group. Impaired energy production or consumption during acute heart failure tended to reflect chronic heart failure. The application of quantitative proteomics based on LTQ OrbiTrap technology effectively evaluated the protein expression in myocardial tissues. In addition to carbohydrates and lipids, other metabolites, including certain amino acids and aldehydes, may also influence energy status.

S100A1 proteins and Ca^{2+}. The present study detected the expression of 12 Ca^{2+}-binding proteins in the myocardial tissues. Of these proteins, 7 were upregulated and 5 downregulated in the Ad-S100A1 EGFP group compared with the control group. The majority of the upregulated proteins, including EF hand domain-containing protein and gelsolin, are important for cardiac muscle contraction, muscle filament sliding and vascular tone modulation. The current study also detected 22 cytoskeletal proteins, 16 of which were upregulated in the Ad-S100A1 EGFP group compared with the control group. These cytoskeletal proteins, including myosin binding protein, myosin 11, myosin 3, and troponin I, are closely associated with Ca^{2+}. The majority of the upregulated proteins are important for electron transport in muscle contraction, cellular Ca^{2+} ion homeostasis, actin filament capping, actin filament severing and actin filament polymerization. Ca^{2+} acts as a global second messenger involved in numerous cellular processes. Ca^{2+} is a vital regulator of muscle contraction and energy production, and modulates various other cellular functions, including secretion and transcription coupling, synaptic transmission, hormonal regulation, cell cycle control, fertilization and vision (18). In the heart, Ca^{2+} is released from the cytoplasmic Ca^{2+} transients to control important Ca^{2+}-dependent enzymes of the tricarboxylic acid cycle and ATP synthase (complex V of the respiratory chain). Many Ca^{2+}-sensor proteins contain a specific Ca^{2+} binding motif (helix-loop-helix, referred to as the EF hand). Calmodulin (CAM), regarded as the prototypical Ca^{2+}-sensor, has four EF hands, and its associated family members include troponin-C (TnC) and MLCs. The S100 proteins contain two Ca^{2+}-binding motifs, a classical C-terminal EF hand and an S100-specific N-terminal EF hand.

S100A1 protein has high tissue and cell specificity, and is preferentially abundant in the heart. It regulates Ca^{2+} homeostasis, contractile inotropy and energy production. At the molecular level, S100A1 interacts with the cardiac isoforms of RyR2, SERCA2A, phospholamban (PLN), titin and mitochondrial F1-ATP synthase (19,20) in a Ca^{2+}-dependent manner. S100A1 has previously been demonstrated to exert a dual effect via its interaction with RyR2. During systole, the opening of the L-type Ca^{2+} channel (LTCC) triggers SR Ca^{2+} release via RyR2 and SR Ca^{2+} reuptake is conducted by SERCA, whereas the Na^{+}-Ca^{2+}-exchanger (NCX) extrudes Ca^{2+} from the cardiomyocyte to maintain steady-state conditions. It stimulates RyR2 to increase systolic function via the enhancement of CICR from the SR (21). S100A1 interacts with RyR2 and the SERCA-phospholamban-complex. Increasing S100A1 protein levels increases systolic SR Ca^{2+} release via RyR2 without an effect on LTCC activity. Furthermore, inducing closure of RyR2 channels during diastole, S100A1 decreases the Ca^{2+} spark frequency to reduce the leakage of Ca^{2+} from the SR (22). Thus, S100A1 stimulates Ca^{2+} uptake into the SR by directly interacting and stimulating the SERCA2A Ca^{2+}-pump. It also interacts with PLN to repress its inhibitory effect on SERCA2A (20). Both effects significantly increase muscle relaxation via the rapid removal of cytoplasmic Ca^{2+} following contraction.

S100A1 directly interacts with the α- and β-chains of F1-ATPase at the inner mitochondrial membrane to stimulate ATP production in a Ca^{2+}-dependent manner. S100A1 couples cardiac Ca^{2+} cycling with Ca^{2+}-dependent mitochondrial energy production (20). The S100A1/F1-ATPase interference in the mitochondria enhances the generation of cytoplasmic ATP in cardiomyocytes (5). The current study demonstrated that 14 carbohydrate metabolism-associated proteins were upregulated in the Ad-S100A1-EGFP group, including malate dehydrogenase, citrate synthase, succinate dehydrogenase [ubiquinone] iron-sulfur subunit, hexokinase-1, pyruvatecarboxylase and 6-phosphofructokinase. The increase in carbohydrate metabolism-associated proteins may also contribute to the recovery of ventricular contraction function in the Ad-S100A1-EGFP group. S100A1 controls contraction and relaxation via interactions at different target sites. S100A1 functions independently of β-adrenergic receptor effects without increasing heart rate, cardiac hypertrophy, cardiac arrhythmias, myocardial fibrosis or other adverse reactions. The effects of S100A1 in the heart involve cAMP, and the protein kinase A and CAM-dependent kinase-II phosphorylation systems (21), which depend on trans-sarcolemmal Ca^{2+} fluxes. S100A1 does not affect Ca^{2+} entry via dihydropyridine receptors, or efflux via the NCX in forward or reverse mode (22).

cTnI. Tn consists of three subunits whose names indicate their roles: Ca^{2+}-binding TnC; inhibitory TnI; and tropomyosin-binding TnT. cTnI is specifically expressed in the myocardium. cTnI is an essential regulator of sarcomere contraction and relaxation. Together with cTnC and cTnT, cTnI binds different tropomyosin sites on the thin actin filament in response to Ca^{2+} (23). In diastole, when intracellular [Ca^{2+}] is low, cTnI binds at the outer domain of actin to maintain tropomyosin, which blocks myosin-binding sites on the thin filament and prevents force development. In systole, when intracellular [Ca^{2+}] is high, Ca^{2+} binds to cTnC and induces a conformational change. This change results in cTnI release from actin and moves tropomyosin closer to the groove of the actin filament, thus, enabling actin-myosin interactions and cardiomyocyte force development (24). cTnI may be a potential treatment target for heart failure because of its important role in the regulation of heart contraction and relaxation. A previous study examined cTnI phosphorylation in healthy and diseased hearts via the activation of the β-adrenergic receptor pathway. cTnI is a regulator of the Frank-Starling mechanism, which regulates heart function by increasing stroke volume with increased in ventricular filling (end-diastolic volume) (22).

MLC. Essential and regulatory MLCs, which have Ca^{2+}-binding EF hand motifs, bind to the neck region of myosin heavy chains. MLCs modulate the Ca^{2+} sensitivity of cross-bridge cycling to control concerted cardiac contractility. MLCs are important for cardiac and skeletal muscle function. When phosphorylated at a specific serine at position 19 by MLC kinase, MLCs induce conformational changes, stimulate myosin-actin interactions and improve cardiomyocyte contraction (25-27). Furthermore, a unique N-terminal domain of essential MLCs directly binds actin to modulate actin-myosin cross-bridge cycling (28-30). Notably, cardiomyocyte-specific overexpression of the N-terminus of human essential MLC (ELC) in rats leads to enhanced cardiac contractility (30,31). In hypertropy, human ELC partially replaced expression of the MLC 3. The MLC 3-to-ELC isoform shift induced a positive inotropic effect (32). It was previously identified that ventricular ELC is cleaved by caspase-3 at a noncanonical cleavage site (33).

HSP70. HSPs comprise a family of intracellular proteins with cytoprotective function. These proteins are induced by stresses and acute conditions, and have previously been demonstrated as essential molecular chaperones involved in cell survival following stress (34,35). Animal models indicate that HSP70 overexpression protects myocardial tissues against ischemia (36). HSP70 has a protective function during acute stress and in patients with chronic stress (36). It has also been previously demonstrated that HSP70 is associated with ischemia and reperfusion following coronary bypass grafting (37). In an acute coronary infarction animal model, Zhang *et al* (38) transplanted bone marrow cells into the ischemic area. Reverse transcription-polymerase chain reaction demonstrated that following bone marrow transplantation, HSP70 expression was upregulated in cardiomyocytes from the infarction and peri-infarction areas, and acute ischemic cardiac function was improved. Furthermore, in acute myocardial infarction or other stress conditions, the body provides protection to the ischemic myocardium via the increased production of HSP. The level of HSP expression is associated with the degree of myocardial protection following AMI. In the present study, the protein expression of HSP70 was significantly increased in the Ad-S100A1-EGFP group.

The majority of the differentially expressed energy metabolism-associated and Ca^{2+}-binding proteins in the Ad-S100A1-EGFP group following AMI were upregulated. This indicates that energy production and contractile ability were enhanced in the ventricular myocardium of the

Ad-S100A1-EGFP group. Ca^{2+} is crucial for the recovery of myocardial function in S100A1 transgenic rats (2). To the best of our knowledge, the current study is the first proteomic analysis of S100A1-adenoviral overexpression using LTQ OrbiTrap, and the results of the study may provide comprehensive insights into the mechanisms of S100A1 in the recovery of heart function following AMI.

Acknowledgements

The current study was supported by the Medical Science and Technology Development Program of Shandong Province (grant no. 2014WSA01015).

References

1. Willis BC, Salazar-Cantú A, Silva-Platas C, Fernández-Sada E, Villegas CA, Rios-Argaiz E, González-Serrano P, Sánchez LA, Guerrero-Beltrán CE, García N, *et al*: Impaired oxidative metabolism and calcium mishandling underlie cardiac dysfunction in a rat model of post-acute isoproterenol-induced cardiomyopathy. Am J Physiol Heart Circ Physiol 308: H467-H477, 2015.
2. Most P, Pleger ST, Völkers M, Heidt B, Boerries M, Weichenhan D, Löffler E, Janssen PM, Eckhart AD, Martini J, *et al*: Cardiac adenoviral S100A1 gene delivery rescues failing myocardium. J Clin Invest 114: 1550-1563, 2004.
3. Most P, Remppis A, Pleger ST, Löffler E, Ehlermann P, Bernotat J, Kleuss C, Heierhorst J, Ruiz P, Witt H, *et al*: Transgenic overexpression of the Ca2+-binding protein S100A1 in the heart leads to increased in vivo myocardial contractile performance. J Biol Chem 278: 33809-33817, 2003.
4. Boerries M, Most P, Gledhill JR, Walker JE, Katus HA, Koch WJ, Aebi U and Schoenenberger CA: Ca2+ -dependent interaction of S100A1 with F1-ATPase leads to an increased ATP content in cardiomyocytes. Mol Cell Biol 27: 4365-4373, 2007.
5. Yamasaki R, Berri M, Wu Y, Trombitás K, McNabb M, Kellermayer MS, Witt C, Labeit D, Labeit S, Greaser M and Granzier H: Titin-actin interaction in mouse myocardium: Passive tension modulation and its regulation by calcium/S100A1. Biophys J 81: 2297-2313, 2001.
6. Most P, Bernotat J, Ehlermann P, Pleger ST, Reppel M, Börries M, Niroomand F, Pieske B, Janssen PM, Eschenhagen T, *et al*: S100A1: A regulator of myocardial contractility. Proc Natl Acad Sci USA 98: 13889-13894, 2001.
7. Most P, Boerries M, Eicher C, Schweda C, Völkers M, Wedel T, Söllner S, Katus HA, Remppis A, Aebi U, *et al*: Distinct subcellular location of the Ca2+-binding protein S100A1 differentially modulates Ca2+-cycling in ventricular rat cardiomyocytes. J Cell Sci 118: 421-431, 2005.
8. Most P, Seifert H, Gao E, Funakoshi H, Völkers M, Heierhorst J, Remppis A, Pleger ST, DeGeorge BR Jr, Eckhart AD, *et al*: Cardiac S100A1 protein levels determine contractile performance and propensity toward heart failure after myocardial infarction. Circulation 114: 1258-1268, 2006.
9. Pleger ST, Shan C, Ksienzyk J, Bekeredjian R, Boekstegers P, Hinkel R, Schinkel S, Leuchs B, Ludwig J, Qiu G, *et al*: Cardiac AAV9-S100A1 gene therapy rescues post-ischemic heart failure in a preclinical large animal model. Sci Transl Med 3: 92ra64, 2011.
10. Pleger ST, Most P, Boucher M, Soltys S, Chuprun JK, Pleger W, Gao E, Dasgupta A, Rengo G, Remppis A, *et al*: Stable myocardial-specific AAV6-S100A1 gene therapy results in chronic functional heart failure rescue. Circulation 115: 2506-2515, 2007.
11. Ross PL, Huang YN, Marchese JN, Williamson B, Parker K, Hattan S, Khainovski N, Pillai S, Dey S, Daniels S, *et al*: Multiplexed protein quantitation in Saccharomyces cerevisiae using amine-reactive isobaric tagging reagents. Mol Cell Proteomics 3: 1154-1169, 2004.
12. Institute of Laboratory Animal Resources (US). Committee on Care, Use of Laboratory Animals, and National Institutes of Health (US). Division of Research Resources: Guide for the care and use of laboratory animals. 8th edition. National Academies Press, Washington, DC, 2011.
13. Stanley WC, Lopaschuk GD, Hall JL and McCormack JG: Regulation of myocardial carbohydrate metabolism under normal and ischaemic conditions. Potential for pharmacological interventions. Cardiovasc Res 33: 243-257, 1997.
14. Tang B, Li Y, Zhao L, Yuan S, Wang Z, Li B and Chen Q: Stable isotope dimethyl labeling combined with LTQ mass spectrometric detection, a quantitative proteomics technology used in liver cancer research. Biomed Rep 1: 549-554, 2013.
15. Lopaschuk GD, Ussher JR, Folmes CD, Jaswal JS and Stanley WC: Myocardial fatty acid metabolism in health and disease. Physiol Rev 90: 207-258, 2010.
16. Andresen BS, Olpin S, Poorthuis BJ, Scholte HR, Vianey-Saban C, Wanders R, Ijlst L, Morris A, Pourfarzam M, Bartlett K, *et al*: Clear correlation of genotype with disease phenotype in very-long-chain acyl-CoA dehydrogenase deficiency. Am J Hum Genet 64: 479-494, 1999.
17. Raha S and Robinson BH: Mitochondria, oxygen free radicals, disease and ageing. Trends Biochem Sci 25: 502-508, 2000.
18. Carafoli E: Calcium-a universal carrier of biological signals. Delivered on 3 July 2003 at the special FEBS meeting in Brussels. FEBS J 272: 1073-1089, 2005.
19. Heizmann CW, Ackermann GE and Galichet A: Pathologies involving the S100 proteins and rage. Subcell Biochem 45: 93-138, 2007.
20. Most P, Remppis A, Pleger ST, Katus HA and Koch WJ: S100A1: A novel inotropic regulator of cardiac performance. Transition from molecular physiology to pathophysiological relevance. Am J Physiol Regul Integr Comp Physiol 293: R568-R577, 2007.
21. Völkers M, Loughrey CM, Macquaide N, Remppis A, DeGeorge BR Jr, Wegner FV, Friedrich O, Fink RH, Koch WJ, Smith GL and Most P: S100A1 decreases calcium spark frequency and alters their spatial characteristics in permeabilized adult ventricular cardiomyocytes.Cell Calcium 41: 135-143, 2007.
22. Kettlewell S, Most P, Currie S, Koch WJ and Smith GL: S100A1 increases the gain of excitation-contraction coupling in isolated rabbit ventricular cardiomyocytes. J Mol Cell Cardiol 39: 900-910, 2005.
23. Kobayashi T and Solaro RJ: Calcium, thin filaments and the integrative biology of cardiac contractility. Annu Rev Physiol 67: 39-67, 2005.
24. Lehman W and Craig R: Tropomyosin and the steric mechanism of muscle regulation. Adv Exp Med Biol 644: 95-109, 2008.
25. Zhi G, Herring BP and Stull JT: Structural requirements for phosphorylation of myosin regulatory light chain from smooth muscle. J Biol Chem 269: 24723-24727, 1994.
26. Chan JY, Takeda M, Briggs LE, Graham ML, Lu JT, Horikoshi N, Weinberg EO, Aoki H, Sato N, Chien KR and Kasahara H: Identification of cardiac-specific myosin light chain kinase. Circ Res 102: 571-580, 2008.
27. Andreev OA, Saraswat LD, Lowey S, Slaughter C and Borejdo J: Interaction of the N-terminus of chicken skeletal essential light chain 1 with F-actin. Biochemistry 38: 2480-2485, 1999.
28. Timson DJ, Trayer HR and Trayer IP: The N-terminus of A1-type myosin essential light chains binds actin and modulates myosin motor function. Eur J Biochem 255: 654-662, 1998.
29. Timson DJ, Trayer HR, Smith KJ and Trayer IP: Size and charge requirements for kinetic modulation and actin binding by alkali 1-type myosin essential light chains. J Biol Chem 274: 18271-18277, 1999.
30. Abdelaziz AI, Segaric J, Bartsch H, Petzhold D, Schlegel WP, Kott M, Seefeldt I, Klose J, Bader M, Haase H and Morano I: Functional characterization of the human atrial essential myosin light chain (hALC-1) in a transgenic rat model. J Mol Med (Berl) 82: 265-274, 2004.
31. Fewell JG, Hewett TE, Sanbe A, Klevitsky R, Hayes E, Warshaw D, Maughan D and Robbins J: Functional significance of cardiac myosin essential light chain isoform switching in transgenic mice. J Clin Invest 101: 2630-2639, 1998.
32. Morano M, Zacharzowski U, Maier M, Lange PE, Alexi-Meskishvili V, Haase H and Morano I: Regulation of human heart contractility by essential myosin light chain isoforms. J Clin Invest 98: 467-473, 1996.
33. Moretti A, Weig HJ, Ott T, Seyfarth M, Holthoff HP, Grewe D, Gillitzer A, Bott-Flügel L, Schömig A, Ungerer M and Laugwitz KL: Essential myosin light chain as a target for caspase-3 in failing myocardium. Proc Natl Acad Sci USA 99: 11860-11865, 2002.
34. Hightower LE and GuidonPT Jr: Selective release from cultured mammalian cells of heat-shock (stress) proteins that resemble glia-axon transfer proteins. J Cell Physiol 138: 257-266, 1989.

35. Knowlton AA, Eberli FR, Brecher P, Romo GM, Owen A and Apstein CS: A single myocardial stretch or decreased systolic fiber shortening stimulates the expression of heat shock protein 70 in the isolated, erythrocyte-perfused rabbit heart. J Clin Invest 88: 2018-2025, 1991.
36. Trost SU, Omens JH, Karlon WJ, Meyer M, Mestril R, Covell JW and Dillmann WH: Protection against myocardial dysfunction after a brief ischemic period in transgenic mice expressing inducible heat shock protein 70. J Clin Invest 101: 855-862, 1998.
37. Dybdahl B, Wahba A, Lien E, Flo TH, Waage A, Qureshi N, Sellevold OF, Espevik T and Sundan A: Inflammatory response after open heart surgery: Release of heat-shock protein 70 and signaling through toll-like receptor-4. Circulation 105: 685-690, 2002.
38. Zhang S, Guo J, Zhang P, Liu Y, Jia Z, Feng X, Li Z, Li W, Ma K, Zhou C and Li L: Transplantation of bone marrow cells up-regulated the expressions of HSP32 and HSP70 in the acute ischemic myocardium. Beijing Da Xue Xue Bao 35: 476-480, 2003 (In Chinese).